Ground-Based Remote Sensing of Total Columnar CO_2, CH_4, and CO Using EM27/SUN FTIR Spectrometer at a Suburban Location (Shadnagar) in India and Validation of Sentinel-5P/TROPOMI

Vijay Kumar Sagar, Mahesh Pathakoti, Mahalakshmi D.V., Rajan K.S., *Member, IEEE*, Sesha Sai M.V.R., Frank Hase, Darko Dubravica, and Mahesh Kumar Sha

***Abstract*— Greenhouse gases (GHGs) play an important role in controlling local air pollution as well as climate change. In this study, we retrieved column-averaged dry-air (X) mole fractions of carbon dioxide (CO_2), methane (CH_4), and carbon monoxide (CO) using a ground-based EM27/SUN Fourier transform infrared spectrometer (FTIR). The EM27/SUN spectrometers are widely in use in the COllaborative Carbon Column Observing Network (COCCON). The PROFFAST software provided by COCCON has been used to analyze the measured atmospheric solar absorption spectra. In this letter, the diurnal variation and the time series of daily averaged XCO$_2$, XCH$_4$, and XCO covering the period from December 2020 to May 2021 are analyzed. The maximum values of XCO$_2$, XCH$_4$, and XCO are observed to be 420.57 ppm, 1.93 ppm, and 170.40 ppb, respectively. Less diurnal but clear seasonal changes are observed during the study period. XCH$_4$ and XCO from the Sentinel-5Precursor (S5P)/TROPOspheric Monitoring Instrument (TROPOMI) are compared against the EM27/SUN retrievals. The correlation coefficient for the EM27/SUN retrieved XCH$_4$ and XCO, with the S5P/TROPOMI products, are 0.75 and 0.94, respectively.**

***Index Terms*— EM27/SUN, greenhouse gases (GHGs), Sentinel-5Precursor (S5P)/TROPOspheric Monitoring Instrument (TROPOMI).**

Manuscript received February 7, 2022; revised April 6, 2022; accepted April 26, 2022. Date of publication April 29, 2022; date of current version May 17, 2022. This work was supported in part by the "National Information system for Climate and Environment Studies (NICES) Programme of ISRO" and in part by the Land-Ocean-Atmospheric GHGs Interaction Experiments (LOAGIN-X) Project of ISRO-Geosphere-Biosphere Programme (ISRO-GBP). *(Corresponding author: Mahesh Pathakoti.)*

Vijay Kumar Sagar, Mahalakshmi D.V., and Sesha Sai M.V.R. are with the Earth and Climate Sciences Area, National Remote Sensing Centre, Indian Space Research Organization (ISRO), Hyderabad 500037, India (e-mail: vijaykmsagar@gmail.com; mahameteorology@gmail.com; seshasaimvr@rediffmail.com).

Mahesh Pathakoti is with the Earth and Climate Sciences Area, National Remote Sensing Center, Indian Space Research Organization (ISRO), Hyderabad 500037, India, and also with the Laboratory for Spatial Informatics (LSI), International Institute of Information Technology (IIIT), Hyderabad 500032, India (e-mail: mahi952@gmail.com).

Rajan K.S. is with the Laboratory for Spatial Informatics (LSI), International Institute of Information Technology (IIIT), Hyderabad 500032, India (e-mail: rajan@iiit.ac.in).

Frank Hase and Darko Dubravica are with the Karlsruhe Institute of Technology (KIT), Institute for Meteorology and Climate Research (IMK-ASF), 76344 Karlsruhe, Germany (e-mail: frank.hase@kit.edu; darko.dubravica@kit.edu).

Mahesh Kumar Sha is with the Royal Belgian Institute for Space Aeronomy (BIRA-IASB), 1180 Brussels, Belgium (e-mail: mahesh.sha@aeronomie.be).

Digital Object Identifier 10.1109/LGRS.2022.3171216

I. Introduction

ANTHROPOGENIC activities entail the release of various trace gases into the atmosphere, mainly due to industrialization, acceleration of economy, and power generation [1]. Though there are many greenhouse gases (GHGs), atmospheric carbon dioxide (CO_2) and methane (CH_4) are the leading contributors to anthropogenic global warming [2]. In India, the total emissions rose to 2.52 Gt CO_2 year^{-1} in 2021 compared to the emissions (2.32 Gt CO_2 year^{-1}) in 2014. Coal fire-based power generation is a major anthropogenic activity contributing about 54% of the electricity produced in India [3]. Due to its steady growth in the atmosphere and uncertainty of source/sink, anthropogenic CH_4 concentration has attracted the interest of the research community over the last decade [4]. Long-term measurements from the National Oceanic and Atmospheric Administration (NOAA) reveal an annual CH_4 increase of 8 ppb·year^{-1} [5] while Shadnagar, the present study site, showed 10 ppb·year^{-1} [6]. Carbon monoxide (CO) is an ozone precursor gas that also affects climate due to its role in the formation of OH radicals in the atmosphere [7]. CO is emitted mostly as a result of incomplete combustion in urban/industrial fossil fuel, biofuel, and biomass combustion. Global CO_2 and CH_4 column measurements are especially useful for understanding regional sources and sinks [8], [9]. The satellite-based XCO$_2$ data with accuracy and precision of 1–2 ppm has the potential to improve the understanding of surface fluxes [10]. At present, several GHG dedicated missions are in orbit, namely the Greenhouse Gases Observing Satellite (GOSAT-1 [11], [12], GOSAT-2 [13], the Orbiting Carbon Observatory-2 (OCO-2), and OCO-3 [8], [9]), and the Copernicus Sentinel-5 Precursor (S5P)/TROPOspheric Monitoring Instrument (TROPOMI) [14]. As a result, combining ground- and space-based remote sensing has become a potent tool for studying GHG spatial and temporal variability. The most important source of GHG reference validation data is the ground-based Fourier transform infrared (FTIR) from the Total Carbon Column Observing Network (TCCON) [15], which has been recently complemented by the portable EM27/SUN FTIR spectrometers from COllaborative Carbon Column Observing Network (COCCON) [16]. The measured near-infrared spec-

tra are used to calculate dry-air column-averaged trace gas abundances.

In the tropics, columnar observations of GHGs are especially important since convection is always prevalent, and as a result, flux patterns are only weakly visible in surface measurements. In this work, solar spectra collected at National Remote Sensing Centre (NRSC), Shadnagar (latitude: 17.036°N; longitude: 78.185°E, and altitude: 500 m a.s.l), a suburban site in India using an EM27/SUN spectrometer, are presented and discussed. This study also includes a comparison of the S5P/TROPOMI $X\mathrm{CH_4}$ and $X\mathrm{CO}$ products with ground-based retrievals of $X\mathrm{CH_4}$ and $X\mathrm{CO}$ during the study period.

II. Data and Methodology

A. EM27/SUN

The spectrometer has been developed by the Karlsruhe Institute of Technology, Germany, in collaboration with Bruker Optics as described in [16]. It covers a spectral range of 4000–10 000 $\mathrm{cm^{-1}}$ (1.0−2.5 μm) with a spectral resolution of ∼0.5 $\mathrm{cm^{-1}}$(maximum optical path difference amounts to 1.8 cm). It records near-infrared solar spectra using an indium gallium arsenide (InGaAs) detector. While $X\mathrm{CO_2}$ and $X\mathrm{CH_4}$ are covered by the main (shortwave) detector, $X\mathrm{CO}$ is covered by the auxiliary (longwave) detector [17]. We have used PROFFAST [18], which is a nonlinear least-square spectral fitting algorithm to retrieve the species concentrations. The spectral windows for $\mathrm{CO_2}$, $\mathrm{CH_4}$, and CO are 6173–6390, 5897–6145, and 4233–4290 $\mathrm{cm^{-1}}$, respectively.

During the study period, a total of 19494 observations were taken from December 7, 2020, to May 3, 2021, covering 74 clear sky days from morning 09:20 Indian Standard Time (IST) to evening 16:45 IST. Preprocessing and trace gas retrievals followed by postprocessing are the two processes in the data analysis chain. The DC correction, fast Fourier transformation, including a phase correction scheme, and a spectral resampling are performed first for generating spectra from the raw interferograms. The retrieval code can take into account instrument-specific deviations from the nominal instrumental line shape (ILS), described by the parameter modulation efficiency amplitude (MEA) and phase error (PE). The parameter MEA measures the deviations of the ILS width from nominal expectation (MEA < 1: broadening, MEA > 1: narrowing), and the parameter PE measures the asymmetry of the ILS [19]. In the framework of COCCON centralized activities, results for MEA and PE parameters for the COCCON EM27/SUN spectrometers are reported by Frey *et al.* [16] and Alberti *et al.* [20]. The average MEA value is 0.983, which has been used in the analysis presented here (together with PE = 0, this being equivalent to the assumption of a symmetrical ILS). In the postprocessing, the retrieved column values are divided by the dry-air column (derived from the co-observed oxygen column) and air mass-independent and air mass-dependent corrections are taken into account for generating the final X_{gas} values. The initial volume mixing ratios files were provided by TCCON (referred to as map files), which contain the *a priori* mixing ratio profiles of the relevant gases, and the temperature profiles were used for the trace gas analysis. The column-averaged amount of dry air (Xair), which measures the instrument's stability, is found to be 0.988 ± 0.008 during the study period. The relative change of Xair was found to be 0.69%, indicating excellent stability of the spectrometer over the observation period.

TABLE I
Details of $X\mathrm{CO_2}$, $X\mathrm{CH_4}$, and $X\mathrm{CO}$ Used During the Study Period

Parameters	Data sources	Resolution	DOI
$X\mathrm{CO_2}$, $X\mathrm{CH_4}$, and $X\mathrm{CO}$	EM27/SUN S. No. 127578552018E044240101	Point location (17.0365° N, 78.1851° E, 540 m)	NA
$X\mathrm{CH_4}$	S5P L2 version 01.04.00	5.5 km x 7 km	[24]
$X\mathrm{CO}$	S5P L2 version 01.04.00	5.5 km x 7 km	[25]

B. Sentinel-5P Retrieved XCH_4 and XCO

Sentinel-5P/TROPOMI instrument was switched to a better spatial resolution of 5.5 km (along-track) × 7 km (across-track) from August 6, 2019. For CO, the processing baseline, product versions, and quality limitations are described in the Product Readme File (PRF) [21]. We have used TROPOMI CO associated with a quality assurance value (qa_value) > 0.5 as recommended in PRF. These criteria separated the retrievals performed under clear sky and clear sky like observations (qa_value = 1, Cloud optical thickness < 0.5 and cloud height < 500 m) and cloudy conditions (qa_value = 0.7, Cloud optical thickness ≥ 0.5, and cloud height < 5000 m). S5P L2 used in the study provides a total vertically integrated column of CO ($\mathrm{TC_{CO}}$), and therefore $X\mathrm{CO}$ is calculated by taking the ratio of $\mathrm{TC_{CO}}$ and a total vertically integrated column of dry air ($\mathrm{TC_{dry\,air}}$). Since the total column of $\mathrm{O_2}$ and $\mathrm{N_2}$ is not available, $\mathrm{TC_{dry\,air}}$ is calculated from the surface pressure (P_s) and vertically integrated water column ($\mathrm{TC_{H2O}}$) from the following equation:

$$X\mathrm{CO} = \frac{\mathrm{TC_{CO}}}{\mathrm{TC_{dry\,air}}} = \frac{\mathrm{TC_{CO}}}{P_s/(g \times m_{\mathrm{dry\,air}}) - \mathrm{TC_{H_2O}} \times (m_{\mathrm{H_2O}}/m_{\mathrm{dry\,air}})} \quad (1)$$

where $g = 9.82\ \mathrm{m{\cdot}s^{-2}}$ is the column-average gravity acceleration and $m_{\mathrm{H2O}} = 0.01801528\ \mathrm{kg{\cdot}mol^{-1}}$ is the molecular mass of $\mathrm{H_2O}$, and $m_{\mathrm{dry,air}} = 0.0289644\ \mathrm{kg{\cdot}mol^{-1}}$ is the molecular mass of dry air [22]. The S5P pixels within the radius of 100 km around the observation site are taken for comparison. The EM27/SUN spectrometer observations are taken within an hour of the satellite overpass. In the same way, the radius of 100 km was taken for the comparison of $\mathrm{CH_4}$ [21], [22]. We have used TROPOMI $X\mathrm{CH_4}$ biased corrected data associated with a quality assurance value (qa_value > 0.5) similar to S5P CO as recommended in $\mathrm{CH_4}$ PRF [23]. The S5P $\mathrm{CH_4}$ is already given in volume mixing ratio and hence compared directly against EM27/SUN retrieved $X\mathrm{CH_4}$. Details of the data used in this study are summarized in Table I.

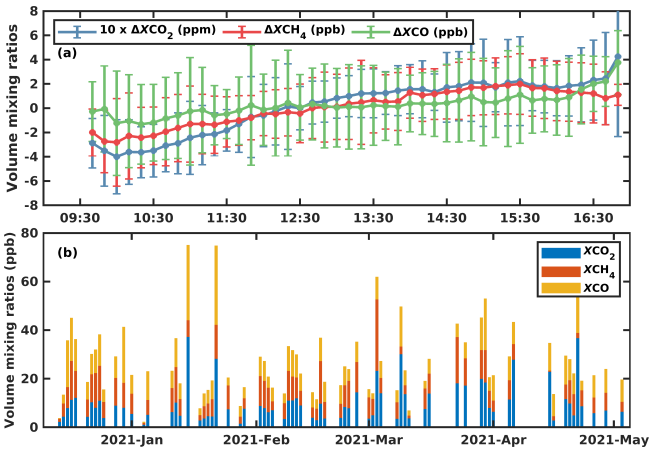

Fig. 1. (a) Daily variation of ΔXCO_2, ΔXCH_4, and ΔXCO during the study period with ± 1 standard deviation (σ). (b) Daily amplitude of XCO_2, XCH_4, and XCO.

TABLE II
STATISTICS OF XCO_2, XCH_4, AND XCO DURING THE STUDY PERIOD

Parameter	Mean±1 σ	Min	Max	Median
XCO_2 (ppm)	415.57±1.89	413.09	420.57	414.78
XCH_4 (ppm)	1.904±0.008	1.882	1.931	1.902
XCO (ppb)	118.74±13.85	94.62	170.40	114.95

III. RESULTS AND DISCUSSIONS

A. Diurnal Variation

Fig. 1 shows the diurnal variability of the deviations (Δ) of XCO_2, XCH_4, and XCO computed after subtracting the daily mean and averaged to 10-min bins across the study period. The daily magnitude of deviation in XCO_2, XCH_4, and XCO are shown in the bottom panel. During different diurnal times, XCO_2 variability range from 0.20 to 1.80 ppm, indicating that XCO_2 has a smaller diurnal variation. When compared to XCO_2, however, XCO has a higher diurnal variation. The major sources of CO are the oxidation of CH_4 and industrial activities such as the combustion process, biomass burning, and the oxidation of nonmethane hydrocarbons [26]. The major sink of CO is oxidation with hydroxyl radical (OH). Maximum and minimum XCO_2, XCH_4, and XCO are summarized in Table II.

B. Temporal Variation

The time-series analysis in Fig. 2 shows clear seasonal changes in XCO_2, XCH_4, and XCO [see Fig. 2(a)–(c)] during the study period. The concentrations are higher in the premonsoon season (March–April–May) than in winter (December–January–February). Minimum CO_2 during winter (dry season) can be due to respiratory loss of carbon as decreased temperature and solar radiation during this period inhibit increases in local CO_2 assimilation. As the season changes from winter to premonsoon, CO_2 concentration rises steadily [6]. From winter to premonsoon, XCH_4 shows less seasonality, with a maximum amplitude change of 0.014 ppm. The spatial distribution of surface fluxes and atmospheric

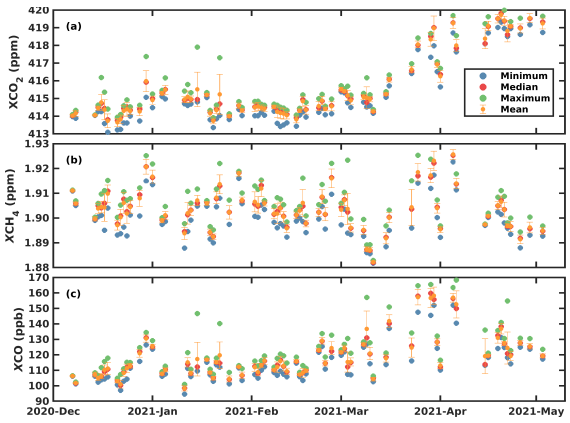

Fig. 2. Daily maximum, minimum, median, and average values with ± 1 σ of (a) XCO_2, (b) XCH_4, and (c) XCO during the study period.

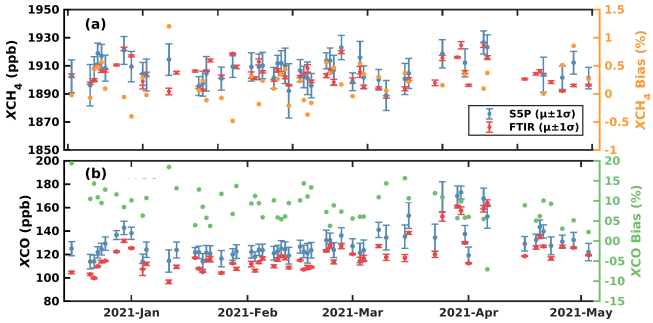

Fig. 3. Time series of the average of EM27/SUN, S5P, and its daily bias percentage (right axis) for (a) XCH_4 and (b) XCO.

transport at the synoptic scale are substantially responsible for the variability of XCO_2 and XCH_4. With an amplitude variation of ~18 ppb, the XCO value indicates considerable seasonality across the study period. In comparison to winter, there is a higher surge in fire activity during the premonsoon season, which could lead to higher atmospheric concentrations. S5P/TROPOMI XCH_4 and XCO were validated from November 2017 to September 2020 against the TCCON and Infrared Working Group of the Network for the Detection of Atmospheric Composition Change (NDACC-IRWG) observations [21].

C. Validation of Sentinel-5P/TROPOMI

In this work, a comparison of S5P/TROPOMI retrieved XCH_4 and XCO with EM27/SUN spectrometer retrievals at Shadnagar is performed. During the study period, spatially and temporally collocated XCH_4 and XCO data from S5P/TROPOMI are compared using a 100 km radius from the observational site and time interval $\pm$ 1 h as criteria. The resultant comparison is shown in Fig. 3(a) and (b) for XCH_4 and XCO.

The average XCH_4 value for EM27/SUN spectrometer and S5P/TROPOMI were found to be 1903.59 $\pm$ 8.46 and 1907.20 $\pm$ 8.45 ppb, respectively, with a bias of 3.61 ppb (0.19%) with the colocated observations. The biases show a high scatter during the winter period. The average XCO

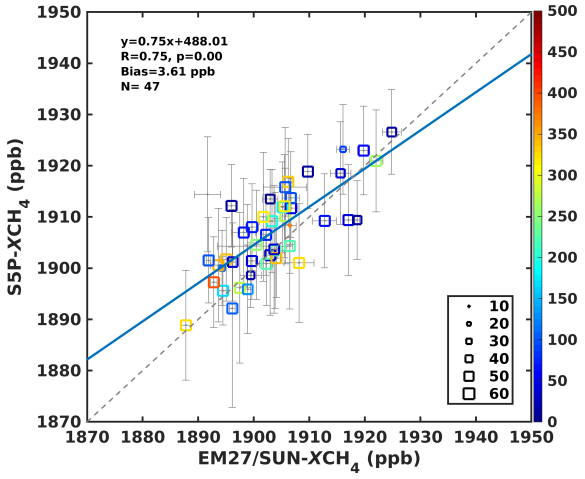

Fig. 4. $X\mathrm{CH_4}$ comparison between S5P/TROPOMI and EM27/SUN. The color bar and the size of the squares represent the number of S5P total column observations and the number of EM27/SUN ground observations at the same time. The horizontal and vertical bar is $\pm 1\sigma$ of S5P and EM27/SUN observations.

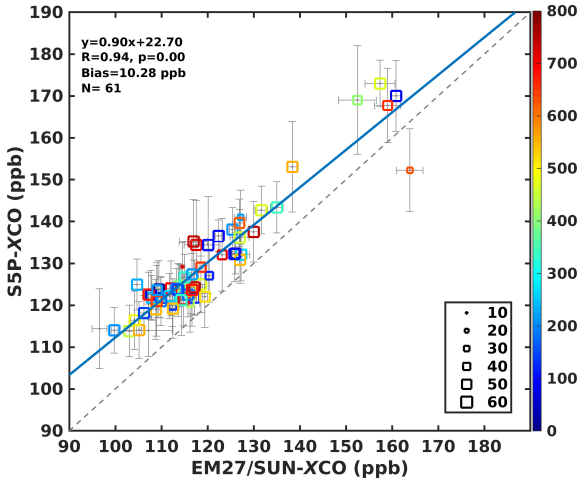

Fig. 5. $X\mathrm{CO}$ comparison between S5P/TROPOMI and EM27/SUN similar to Fig. 4.

values for EM27/SUN and S5P/TROPOMI were found to be 119.46 ± 14.57 and 129.72 ± 14.01 ppb, respectively, with a bias of 10.26 ppb (8.59%). The bias during the winter period is high and on a few days exceeds over 15%. The bias values go down during the April–May period showing signs of seasonality. The comparative analysis of $X\mathrm{CH_4}$ and $X\mathrm{CO}$ from EM27/SUN spectrometer and S5P/TROPOMI showed high positive correlation coefficients (r) of 0.75 and 0.94, respectively (see Figs. 4 and 5). Thus, we report a good agreement between retrievals of $X\mathrm{CH_4}$ and $X\mathrm{CO}$ from EM27/SUN and S5P/TROPOMI retrievals.

In order to verify the effect of local conditions (topography, surface albedo, sources of target gases, etc.), we did a sensitivity study, where we varied the colocation radius criterion from 10 to 100 km in steps of 10 km radii. Fig. 6(a) and (b) shows the average of all S5P pixels around the site location. High values of $\mathrm{CH_4}$ and CO can be seen around the city of Hyderabad (with over 10.5 million population). Fig. 6(c) and (d) shows

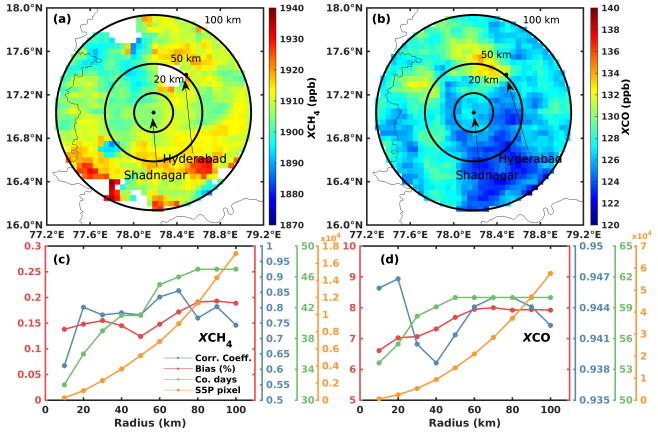

Fig. 6. (a) Representation of S5P observations under an area of 100 km radius, the inner circles represent the 50 and 20 km radius, for all observations during the study period centered at the site for $X\mathrm{CH_4}$ and (b) $X\mathrm{CO}$, (c) bias in percentage (left axis), the r value, number of coincident observation days and the total number of S5P pixels (right axis) in the different radius of area for $X\mathrm{CH_4}$, and (d) $X\mathrm{CO}$.

that selecting small radii for colocation limits the number of colocation days and pixels resulting in low correlation and high scatter. However, as the radii are increased, the statistics get more robust and the change in the parameters becomes small. In the case of a specific application, it may be interesting to select a radius of <50 km to keep out the pixels covering the city of Hyderabad.

IV. Conclusion

In this study, we demonstrated first-hand $X\mathrm{CO_2}$, $X\mathrm{CH_4}$, and $X\mathrm{CO}$ measurements using the EM27/SUN spectrometer data from December 7, 2020, to May 3, 2021. During this study period, the dry-air column was observed to be in the range of 0.985–0.992, indicating the stability of the EM27/SUN spectrometer. $X\mathrm{CO_2}$, $X\mathrm{CH_4}$, and $X\mathrm{CO}$ exhibited mild diurnal variation. The retrieved columnar concentrations also observed clear seasonality from winter to premonsoon. Furthermore, this study evaluated Sentinel 5P/TROPOMI retrieved $X\mathrm{CH_4}$ and $X\mathrm{CO}$ against EM27/SUN spectrometer retrievals and found very good agreement with r values of 0.74 and 0.94, respectively. The biases between EM27/SUN and S5P/TROPOMI retrieved $X\mathrm{CH_4}$ and $X\mathrm{CO}$ are 3.61 ppb (0.19%) and 10.26 (8.59%), respectively, meeting mission requirements of bias ± precision of less than 1.5% ± 1% for $\mathrm{CH_4}$ and 15% ± 10% for CO. Thus, this study demonstrated the retrievals of $X\mathrm{CO_2}$, $X\mathrm{CH_4}$, and $X\mathrm{CO}$ while meeting the COCCON observations along with satellite validation.

Acknowledgment

The authors would like to thank Dr. Prakash Chauhan, Director, NRSC, and Dr. Raj Kumar, former Director, NRSC, for their kind encouragement and support to carry out this work. The authors would like to acknowledge COCCON for PROFFAST software and extend their guidance in retrieving the data. They sincerely thank the editor and anonymous reviewers for the constructive

comments and suggestions, which have certainly helped us to improve the manuscript. They also thank the European Space Agency for the Copernicus S5P/TROPOMI mission data.

REFERENCES

[1] J. G. Canadell *et al.*, "Multi-decadal increase of forest burned area in Australia is linked to climate change," *Nature Commun.*, vol. 12, no. 1, p. 6921, Dec. 2021, doi: 10.1038/s41467-021-27225-4.

[2] T. F. Stocker *et al.*, *Working Group I Contribution to the Fifth Assessment Report of the Intergovernmental Panel on Climate Change*. Cambridge, U.K.: Cambridge Univ. Press, 2013, p. 1535.

[3] *Annual Reports Year Wise (Ministry) | Government of India | Ministry of Power*. Accessed: Jan. 31, 2022. [Online]. Available: https://powermin.gov.in/sites/default/files/uploads/Annual_Report_2010-11_English.pdf

[4] J. Huang, H. Yu, X. Guan, G. Wang, and R. Guo, "Accelerated dryland expansion under climate change," *Nature Climate Change*, vol. 6, no. 2, pp. 166–171, Feb. 2016, doi: 10.1038/nclimate2837.

[5] U.S. Department of Commerce. *Global Monitoring Laboratory—Carbon Cycle Greenhouse Gases*. Accessed: Jan. 31, 2022. [Online]. Available: https://gml.noaa.gov/ccgg/trends_ch4/

[6] G. Sreenivas *et al.*, "Seasonal and annual variations of CO_2 and CH_4 at shadnagar, a semi-urban site," *Sci. Total Environ.*, vol. 819, May 2022, Art. no. 153114, doi: 10.1016/j.scitotenv.2022.153114.

[7] P. J. Crutzen and P. H. Zimmermann, "The changing photochemistry of the troposphere," *Tellus A, Dyn. Meteorol. Oceanogr.*, vol. 43, no. 4, pp. 136–151, Aug. 1991, doi: 10.1034/j.1600-0870.1991.00012.x.

[8] C. Frankenberg *et al.*, "The Orbiting Carbon Observatory (OCO-2): Spectrometer performance evaluation using pre-launch direct sun measurements," *Atmos. Meas. Techn.*, vol. 8, no. 1, pp. 301–313, Jan. 2015, doi: 10.5194/amt-8-301-2015.

[9] A. Eldering *et al.*, "The Orbiting Carbon Observatory-2: First 18 months of science data products," *Atmos. Meas. Techn.*, vol. 10, no. 2, pp. 549–563, 2017, doi: 10.5194/amt-10-549-2017.

[10] P. J. Rayner and D. M. O'Brien, "The utility of remotely sensed CO_2 concentration data in surface source inversions," *Geophys. Res. Lett.*, vol. 28, no. 1, pp. 175–178, Jan. 2001, doi: 10.1029/2000GL011912.

[11] Y. Yoshida *et al.*, "Improvement of the retrieval algorithm for GOSAT SWIR XCO_2 and XCH_4 and their validation using TCCON data," *Atmos. Meas. Techn.*, vol. 6, no. 6, pp. 1533–1547, Jun. 2013, doi: 10.5194/amt-6-1533-2013.

[12] A. Kuze, H. Suto, M. Nakajima, and T. Hamazaki, "Thermal and near infrared sensor for carbon observation Fourier-transform spectrometer on the greenhouse gases observing satellite for greenhouse gases monitoring," *Appl. Opt.*, vol. 48, no. 35, pp. 6716–6733, Dec. 2009, doi: 10.1364/AO.48.006716.

[13] H. Suto *et al.*, "Thermal and near-infrared sensor for carbon observation Fourier transform spectrometer-2 (TANSO-FTS-2) on the greenhouse gases observing SATellite-2 (GOSAT-2) during its first year in orbit," *Atmos. Meas. Techn.*, vol. 14, no. 3, pp. 2013–2039, Mar. 2021, doi: 10.5194/amt-14-2013-2021.

[14] J. P. Veefkind *et al.*, "TROPOMI on the ESA Sentinel-5 precursor: A GMES mission for global observations of the atmospheric composition for climate, air quality and ozone layer applications," *Remote Sens. Environ.*, vol. 120, pp. 70–83, May 2012, doi: 10.1016/j.rse.2011.09.027.

[15] D. Wunch *et al.*, "The total carbon column observing network," *Philos. Trans. Roy. Soc. A, Math., Phys. Eng. Sci.*, vol. 369, no. 1943, pp. 2087–2112, May 2011, doi: 10.1098/RSTA.2010.0240.

[16] M. Frey *et al.*, "Building the Collaborative Carbon Column Observing Network (COCCON): Long-term stability and ensemble performance of the EM27/SUN Fourier transform spectrometer," *Atmos. Meas. Techn.*, vol. 12, no. 3, pp. 1513–1530, Mar. 2019, doi: 10.5194/amt-12-1513-2019.

[17] F. Hase *et al.*, "Addition of a channel for XCO observations to a portable FTIR spectrometer for greenhouse gas measurements," *Atmos. Meas. Tech.*, vol. 9, no. 5, pp. 2303–2313, 2016, doi: 10.5194/amt-9-2303-2016.

[18] M. K. Sha *et al.*, "Intercomparison of low- and high-resolution infrared spectrometers for ground-based solar remote sensing measurements of total column concentrations of CO_2, CH_4, and CO," *Atmos. Meas. Techn.*, vol. 13, no. 9, pp. 4791–4839, Sep. 2020, doi: 10.5194/amt-13-4791-2020.

[19] F. Hase, T. Blumenstock, and C. Paton-Walsh, "Analysis of the instrumental line shape of high-resolution Fourier transform Ir spectrometers with gas cell measurements and new retrieval software," *Appl. Opt.*, vol. 38, no. 15, pp. 3417–3422, 1999.

[20] C. Alberti *et al.*, "Improved calibration procedures for the EM27/SUN spectrometers of the COllaborative Carbon Column Observing Network (COCCON)," *Atmos. Meas. Tech.*, vol. 15, no. 8, pp. 1–48, 2021.

[21] *TROPOMI Level 2 Carbon Monoxide Total Column*, Eur. Space Agency, 2021.

[22] M. K. Sha *et al.*, "Validation of methane and carbon monoxide from Sentinel-5 Precursor using TCCON and NDACC-IRWG stations," *Atmos. Meas. Tech.*, vol. 14, no. 9, pp. 6249–6304, 2021, doi: 10.5194/amt-14-6249-2021.

[23] *TROPOMI Level 2 Methane Total Column*, Eur. Space Agency, 2021.

[24] *Copernicus Sentinel-5P (Processed by ESA), 2019, TROPOMI Level 2 Methane Total Column. Version 01*, Eur. Space Agency, 2019, doi: 10.5270/S5P-3p6lnwd.

[25] *Copernicus Sentinel-5P (Processed by ESA), 2018, TROPOMI Level 2 Carbon Monoxide Total Column. Version 01*, Eur. Space Agency, 2018.

[26] J. H. Seinfeld and S. N. Pandis, "Atmospheric chemistry and physics: From air pollution to climate change," *Environ., Sci. Policy Sustain. Develop.*, vol. 40, no. 7 p. 1149, 1998.